Journal of Power Sources 219 (2012) 60–64

Contents lists available at SciVerse ScienceDirect

Journal of Power Sources

journal homepage: www.elsevier.com/locate/jpowsour

Short communication

Preparation and characterization of hydro-reactive Mg–Al mechanical alloy materials for hydrogen production in seawater

Mei-Shuai Zou*, Xiao-Yan Guo, Hai-Tao Huang, Rong-Jie Yang, Peng Zhang

School of Materials Science and Engineer, Beijing Institute of Technology, Beijing 100081, China

HIGHLIGHTS

- ► Hydro-reactive Mg–Al mechanical alloy materials were prepared by high-energy milling.
- ► Hydrolysis properties and mechanism of Mg–Al alloy materials were studied in seawater.
- ► High-energy ball milling is an efficient method for improving the reactivity of Mg–Al alloy materials in seawater.
- ► Bi and Co as the cathode plays an important role in the hydrolysis of Mg–Al alloy in seawater.

ARTICLE INFO

Article history:
Received 20 May 2012
Received in revised form
29 June 2012
Accepted 1 July 2012
Available online 24 July 2012

Keywords:
Magnesium–aluminum alloy
Hydro-reactive materials
High-energy milling
Hydrolysis reaction
Hydrogen production

ABSTRACT

Hydro-reactive Mg–Al mechanical alloy materials are prepared by high-energy milling. Scanning electron microscopy (SEM), thermogravimetric (TG) and powder X-ray diffraction (XRD) techniques are used to characterize the materials. Their hydrolysis properties are studied in seawater by measuring the hydrogen volume produced and by calculating the rate of hydrogen evolution. The collected reaction products are analyzed after hydrolysis. The experimental results show that there are the squashed, overlapped and fined steps for metal powder in the milling progress. As the milling time increases from 0 to 4 h, the initial oxidization temperature of Mg–Al mechanical alloy materials first increases, and then decreases. An increase in milling time is found to improve the hydrogen generation rate and the hydrogen yield during hydrolysis. When the milling time reaches 4 h, the hydrolysis reaction is immediately noticeable, generating 397 mL(min g)$^{-1}$ of hydrogen within the first second minutes, and the total hydrogen evolution is 950 mL of hydrogen, or 97.1% of the theoretical yield.

1. Introduction

Hydrogen is considered as “the twenty-first century” of green energy owing to its unique features, and many countries are stepping up the deployment of hydrogen-based energy strategy. The fact that the chemical energy of hydrogen can be easily converted to electrical energy using fuel cells such as PEMFCs (proton exchange membrane fuel cells), makes this an extremely attractive strategy.

Although various sources of hydrogen have been studied, including carbon-based H_2, metal hydrides, chemical hydrides, methanol, compressed H_2 and fossil fuels, there are some disadvantages that limit the efficient use of hydrogen, such as its price, pollution, safety and utility [1–5]. Light metals have the potential for use as hydrogen generation materials because they are relatively safe, simple and environmentally friendly sources of high-purity hydrogen [6].

There are a number of metals that react with water, such as magnesium, aluminum, lithium, and beryllium. Considering the potential energy, storage ability, and low toxicity of magnesium and aluminum systems, Mg/H_2O and Al/H_2O systems have potential in this context [7]. Pure hydrogen can be obtained through the following reactions [3,8]:

$$Mg + 2H_2O \rightarrow Mg(OH)_2 + H_2$$

$$2Al + 6H_2O \rightarrow 2Al(OH)_3 + 3H_2$$

Using the above equation, the Al/H_2O system was calculated to have a higher theoretical hydrogen yield than the Mg/H_2O system. Although Al/H_2O has higher energy density than the Mg/H_2O system, it has a lower reactivity because the aluminum oxide film has highly protective properties [9] (Pilling–Bedworth coefficient $\varphi = 1.28$).

Previous reports have demonstrated [10–15] that the ball-milling appears to be a promising route for the hydrolysis of

* Corresponding author. Tel.: +86 (0)10 68913456; fax: +86 (0)10 68914862.
E-mail address: zoumeishuai@gmail.com (M.-S. Zou).

0378-7753/$ – see front matter © 2012 Elsevier B.V. All rights reserved.
http://dx.doi.org/10.1016/j.jpowsour.2012.07.008

metal-based materials. However, there is no report on the hydrolysis of hydro-reactive Mg–Al mechanical alloy materials. According to the reactive characteristics of Al/H_2O and Mg/H_2O [16–19], we chose Co and Bi as the catalysts [14,20], and we prepared the Mg–Al alloy materials using the high-energy ball milling method. The hydrolysis of these highly reactive Mg–Al alloy materials in seawater further improved the release of energy compared with the previously reported pure ball-milled Mg. We believe that this material has great value as the hydrogen source in seagoing power systems.

2. Experimental

The starting materials were elemental magnesium (Mg, 99%); aluminum (Al, 99%); bismuth (Bi, 99%) and cobalt (Co, 99%) powders and seawater.

The magnesium and aluminum were produced in Weihao Company of China, and the average particle size (d50) of them is about 50 μm. The impurities of them include Fe, Si, Cu, etc., and the content of maximum impurity is less than 0.2%. The seawater was directly taken from Beidaihe in China. Bismuth and cobalt powders are analytical grade chemicals.

The milling experiments were performed in a Simoloyer CM01 with a chamber volume of 1 L. The procedure was performed with the addition of 0.5 wt% stearic acid to prevent the metal flakes from adhering to each other or "coating" on the milling tools. An inert atmosphere of argon was used to prevent oxidation. The process parameters for the milling are shown in Table 1. Table 2 shows the compositions of the Mg–Al alloy materials.

The hydrolysis reactions of the Mg–Al alloy materials with seawater were performed in a 100 mL flask reactor that had two openings: a water inlet and a gas outlet. The volume of the hydrogen produced was measured by drainage, and the generation rate was calculated by the amount evolved from the beginning of the test to a given time. The reaction products were collected by filtration and vacuum drying.

Powder X-ray diffraction (XRD) was performed on an X' Pert PRO MPD diffractometer with Cu Kα radiation.

Scanning electron microscopy (SEM) observations were performed using an FE-SEM S4800 microscope.

The size distributions of the powders were determined using the Laser Particle Size Analyzer MS 2000.

Thermogravimetric (TG) analysis of samples were performed on a NETZSCH F209 apparatus at 50–900 °C, in an air atmosphere, at a flowing rate of 30 mL min^{-1} and a heating rate at 10 °C min^{-1}.

3. Results and discussion

3.1. Characterization of the Mg–Al alloy materials at different milling times

3.1.1. Particle morphology

We prepared the Mg–Al alloy materials using the high-energy milling process. SEM images of representative examples at different milling times are shown in Fig. 1. Most of the spherical powder, which was milled for 1 h, became thin and flake-like in structure. As the milling time was increased, superposition of the thin sheets of metal occurred, and the materials gradually began to thicken. Within 4 h of milling, the shapes of the alloy particles were irregular, and the alloy particles formed a multi-layer structure.

Table 1
Milling equipment and parameters.

Ball miller	Simoloyer CM01-21
Milling balls	Material: steel (100Cr6), diameter: 5.1 mm
Powder/ball mass ratio	1:10
Milling atmosphere	Argon
Milling time	1–4 h
Rotary speed	1200 rpm/48 s, 800 rpm/12 s
Operating model	Cycle
Cooling-grinding unit	Water

Table 2
The composition of the Mg–Al alloy materials.

Sample	Mg/wt%	Al/wt%	Co/wt%	Bi/wt%	Milling time/h
Mg–Al blended power	70	30	3	2	0
Mg–Al-1	70	30	3	2	1
Mg–Al-2	70	30	3	2	2
Mg–Al-3	70	30	3	2	3
Mg–Al-4	70	30	3	2	4

3.1.2. Size distributions

The size distribution of the Mg–Al alloy materials at different milling times was determined and is shown in Fig. 2. The milled powder had a wider size distribution than the Mg–Al blended power, and the mechanical alloys contained slightly less of the finest particles than the spherical blended powder. The average size (d(0.5)) of the mechanical alloy particles varied from 54.34 μm to 120.26 μm, and the average size of the spherical blend particles was 29.43 μm (Table 3).

According to the pattern and size change of the Mg–Al alloy materials in the milling process, we propose the existence of squashed, overlapped and fined steps.

3.1.3. The reactivity of Mg–Al alloy materials in air atmosphere

The Mg–Al alloy materials, which were milled for different lengths of time, were investigated using TG to measure their reactivity in air (Fig. 3). According to the results, the milled Mg–Al alloy materials differed from the unmilled Mg–Al blended power by the onset temperature of oxidation. The milled samples had a lower starting oxidation temperature than the unmilled Mg–Al blended powder. However, as the milling time was increased from 0 h to 4 h, the initial oxidation temperature of the milled Mg–Al alloy materials first increased and then decreased. This trend is in accordance with the trend observed in the average-sized powder. Presumably, the smaller-sized powder has a larger specific surface area; thus, it is more readily oxidized.

Once the alloy materials were oxidized, a sharp weight increase was observed from the TG cures. The final mass increase of the Mg–Al alloy materials, each with varying amounts of milling time, was nearly equivalent as the temperature was increased to 900 °C. Because of the temperature limit of the instrument, we were unable to study the higher oxidization temperatures. Nonetheless, the oxidization trends suggest that the mass will further increase as the temperature continues to increase.

3.1.4. Phase structure

Microstructural changes in the ball-milled Mg–Al powders were determined using X-ray diffraction. The X-ray diffraction patterns showing the evolution of their structure are shown in Fig. 4. The initial Mg–Al blended powder clearly shows both Mg and Al peaks. Additionally, there are no major changes in the diffraction peaks for the Mg and Al peaks for milled Mg–Al alloy materials, which revealed that the Mg–Al was only to generate plug-in solid solution in the milling process. However, the diffraction peaks that are characteristic of Mg–Al alloy materials appear to noticeably broaden as the milling time increased. This result indicates that the crystallite size of Mg–Al alloy materials decreased

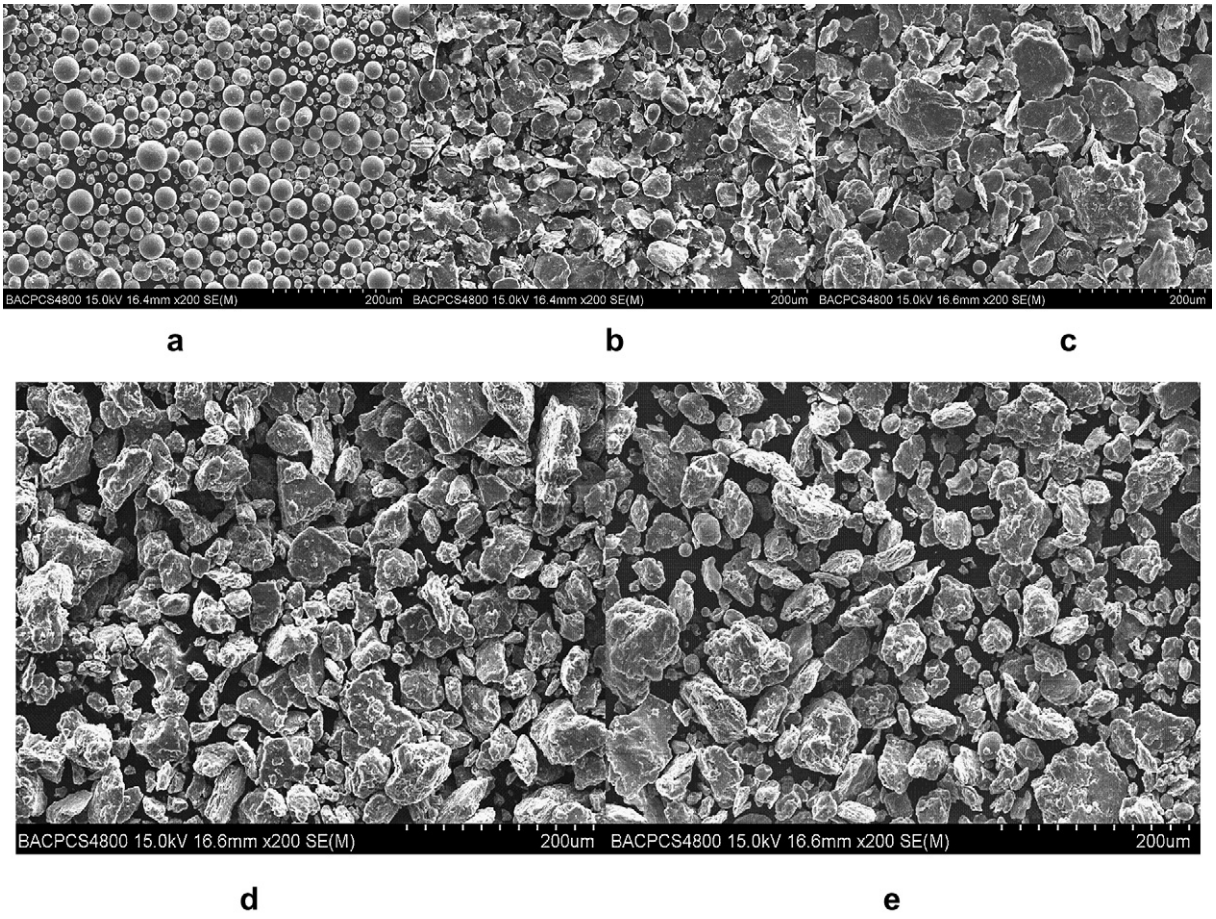

Fig. 1. SEM of Mg–Al alloy materials as a function of different milling times: (a) 0 h, (b) 1 h, (c) 2 h, (d) 3 h, (e) 4 h.

during the high-energy milling due to the repeated grain break-up, cold welding and re-welding [21].

The new diffraction peaks of the Mg–Al alloy materials before the 30° diffraction angle in the milling process were attributed to the formation of composites from an excess of magnesium with the catalyst.

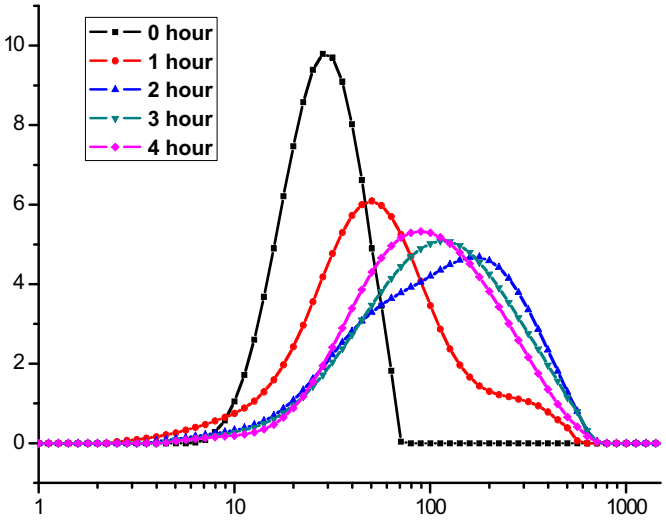

Fig. 2. The size distributions of Mg–Al alloy materials.

3.2. Hydrolysis properties and mechanism of Mg–Al alloy materials

The hydrolysis properties of the Mg–Al mechanical alloy materials in seawater at various milling times were studied, and the data for hydrogen evolution at room temperature are shown in Table 4.

The Mg–Al blended powder barely reacted with seawater, evolving only 11 mL of hydrogen over a long time period. This phenomenon was attributed to the structure of the blended powder and to the stability of the metal oxide film on its surface. Another reason for this low reactivity may be the formation of a passive metal hydroxide layer on the surface of the metal powder in its reaction with seawater [7].

When the Mg–Al alloy materials reacted with seawater, the hydrolysis reaction was immediately noticeable. Increased milling time improved the hydrogen generation rate and hydrogen yield. When the mixture was milled for 1 h, the hydrolysis reaction rate was 34 mL(min g)$^{-1}$ within the first 2 min, and the rate began to accelerate along with the reaction. However, the hydrogen yield was only 64.28% of the theoretical yield. When the mixture was milled for 4 h, the hydrolysis reaction was immediately noticeable, generating 397 mL(min g)$^{-1}$ within the first second minutes. The

Table 3
The average size of Mg–Al alloy materials.

Milling time/h	0	1	2	3	4
$d(0.5)/\mu m$	29.43	54.34	120.26	113.13	98.81

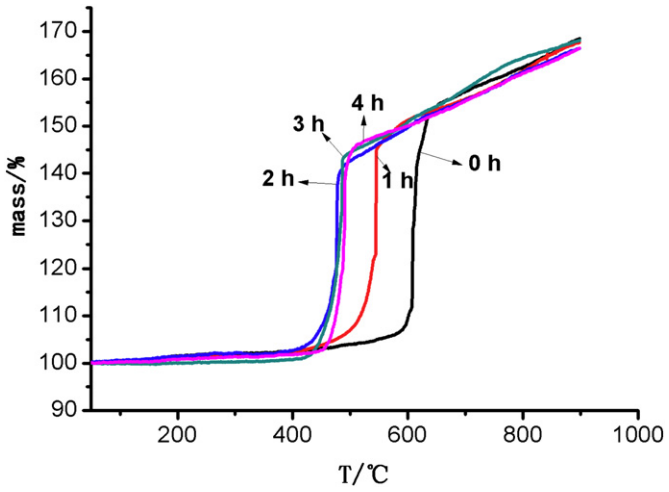

Fig. 3. TG cures of Mg–Al alloy materials in air atmosphere.

total hydrogen evolution was 950 mL, or 97.2% of the theoretical yield.

After the hydrolysis of the Mg–Al-4 alloy materials, the solid hydrolysis products were collected by filtering filtration and were dried under vacuum. XRD patterns (Fig. 4) were then fitted to analyze the phase compositions in the reaction products to study the hydrolysis mechanism.

First, the elemental Mg or Al peaks were absent, suggesting that the Mg or Al content of the hydrolysis products was below the detection limit of the instrument. From this analysis and the total amount of hydrogen evolved (listed in Table 4), we concluded that the reaction of the Mg–Al-4 alloy materials with seawater proceeded almost completely. Second, we observed small crystal peaks that corresponded to $Mg(OH)_2$, which is the result of excess magnesium that had reacted with seawater. There were no $Al(OH)_3$ peaks in the hydrolysis products, suggesting that single Al did not react with seawater in Mg–Al-4 alloy materials. However, there are several unformed peaks in Fig. 4. We infer that these unformed peaks were due to the formation of Al–Mg-based amorphous compounds, unlike crystal aluminum hydroxide, which could inhibit the reaction of metal with water due to its dense oxide [9].

Bi was clearly observed from the XRD pattern, which suggests that Bi did not participate in the reaction. And Co in the hydrolysis product was not able to be measured due to the low content and more absorption of Co to Cu K_α-ray [22].

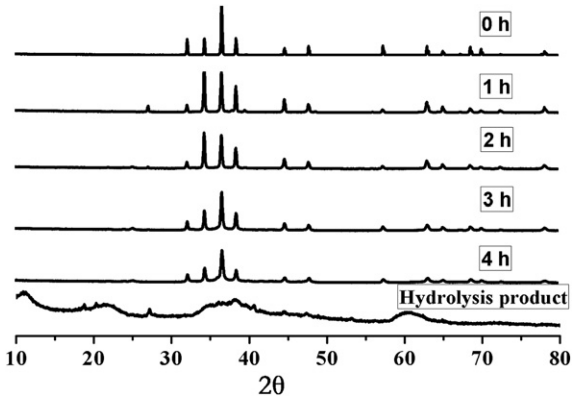

Fig. 4. The XRD of Mg–Al alloy materials in different milling times.

Table 4
Data of hydrogen evolution in the reaction of Mg–Al with seawater.

Milling time/h		0	1	2	3	4
Reactive rate/mL(min g)$^{-1}$	0–2 min	0	34	142	321	397
	2–10 min	0.5	39	45	33.5	19.5
	10–20 min	0.4	21	34	10	0
Total reaction time/min		120	20	16	11	8
Total produced H_2/mL		11	628	845	920	950
Conversion yield/%		1.25	64.28	86.49	94.16	97.2

According to the above analysis, we can infer certain things about the hydrolysis of Mg–Al alloy materials. First, the elimination of the oxide layer by mechanical milling improved the reaction rate. Second, surface defects were created in the metal surface by milling. Numerous defects and fresh surfaces accentuated the pitting corrosion in the presence of Cl^- [17]. Third, Bi and Co as the cathode played an important role in the hydrolysis of Mg–Al alloy due to their low hydrogen overpotentials. In other words, water was reduced by obtaining electrons in the cathode, and the Mg–Al alloy lost electrons at the anode in this hydrolysis process [23]. Finally, the formation of Al–Mg-based amorphous compounds, unlike the dense metal oxide, further improved the efficiency of the reaction. In addition, the heat released from the reaction of excess magnesium with seawater may have promoted the Mg–Al alloy system hydrolysis.

4. Conclusions

High-energy ball milling is an efficient method for improving the reactivity of Mg–Al alloy materials in seawater, and squashed, overlapped and fined steps exist in the milling progress. Consequently, the high-energy ball milling process has a great influence on the performance of Mg–Al based hydro-reactive materials.

In summary, we have demonstrated important benefits of the Mg–Al mechanical alloy for hydrolysis. Specifically, Mg–Al-4 hydro-reactive materials have excellent hydrolysis performance and could react completely with seawater in a short time.

These results show the feasibility for the utilization of Mg–Al hydro-reactive materials in the production of green energy.

Acknowledgments

This work was financially supported by the National Natural Science Foundation of China, the Youthful Fund of Power and the Detonator Industry in China.

References

[1] Susana Silva Martinez, Loyda Albanil Sanchez, Alberto A. Alvarez Gallegos, P.J. Sebastian, International Journal of Hydrogen Energy 32 (2007) 3159–3162.
[2] J.M. Olivares-Ramirez, R.H. Castellanos, A. Marroquin de Jesus, E. Borja-Arco, R.C. Pless, International Journal of Hydrogen Energy 33 (2008) 2620–2626.
[3] Takehito Hiraki, Tomohiro Akiama, International Journal of Hydrogen Energy 34 (2009) 153–161.
[4] Lluis Soler, Jorge Macanas, Maria Munoz, Juan Casado, Journal of Power Sources 169 (2007) 144–149.
[5] Y. Kojima, E.-I. Suzuki, K. Fukumotoa, Y. Kawai, Masahiko Kimbara, Haruyuki Nakanishi, Shinichi Matsumoto, Journal of Power Sources 125 (2004) 22–26.
[6] T. Hiraki, S. Yamauchi, R. Fukuzato, T. Akiyama, CAMP-ISIJ 18 (2005) 261.
[7] M.S. Zou, R.J. Yang, X.Y. Guo, H.T. Huang, J.Y. He, P. Zhang, International Journal of Hydrogen Energy 36 (2011) 6478–6483.
[8] M.H. Grosjean, M. Zidoune, L. Roue, Journal of Alloys and Compounds 404–406 (2005) 712–715.
[9] A.L. Breiter, V.M. Mal'tsev, E.I. Popov, Combustion, Explosion, and Shock Waves 13 (1977) 475–485.

[10] Zhongwei Zhao, Xingyu Chen, Mingming Hao, Energy 36 (2011) 2782–2787.
[11] Tomasz Troczynski, Vancouver, Edith Czeth, North Vancouver, US 0232837, 2005.
[12] M.H. Grosjean, M. Zidoune, L. Roue, J.Y. Huot, International Journal of Hydrogen Energy 31 (2006) 109–119.
[13] Paul Dupiano, Demitrios Stamatis, Edward L. Dreizin, International Journal of Hydrogen Energy 36 (2011) 4781–4791.
[14] Mei-Qiang Fan, Fen Xu, Li-Xian Sun, Jun-Ning Zhao, T. Jiang, Wei-Xun Li, Journal of Alloys and Compounds 460 (2008) 125–129.
[15] Mei-Qiang Fan, Fen Xu, Li-Xian Sun, International Journal of Hydrogen Energy 32 (2007) 2809–2815.
[16] Guang Ling Song, Andrej Atrens, Advanced Engineering Materials 1 (1999) 11–33.
[17] J. Skrovan, A. Alfantazi, T. Troczynski, Journal of Applied Electrochemistry 39 (2009) 1695–1702.
[18] B.C. Bunker, G.C. Nelson, K.R. Zavadil, J.C. Barbour, F.D. Wall, J.P. Sullivan, Journal of Physical Chemistry B 106 (2002) 4705–4713.
[19] Vladimir I. Kirillov, St. Petersburg Petrodvoretz, Alexander N. Vastrebov, St. Petersburg, US 5494538, 1996.
[20] Adriana N. Correia, Sergio A.S. Machado, Luis A. Avaca, Electrochemistry Communications (1999) 600–604.
[21] E. Czech, T. Trocynski, International Journal of Hydrogen Energy 35 (2010) 1029–1037.
[22] Sun Jianfei, Zhang Faming, Shen Jun, Xian Hengze, Chinese Journal of Rare Metals 27 (2003) 665–670.
[23] Karl Hohne, Erlangen, US 3985865, 1976.